Indian Journal of Geo Marine Sciences
Vol. 51 (05), May 2022, pp. 484-489
DOI: 10.56042/ijms.v51i05.65575

Batch kinetic studies of adsorption of Cu(II) ions from aqueous solutions onto alginate nanoparticles/PEG binary blend

M Saranya, T Gomathi*, S Pavithra, A Mubashirunnisa & P N Sudha

PG and Research Department of Chemistry, D.K.M. College for Women, Vellore, Tamil Nadu – 632 001, India

*[E-mail: chemist.goms@gmail.com]

Received 07 February 2022; revised 10 May 2022

Among the most prevalent natural biopolymers is alginate. The current effort focuses on creating the binary blend of Alg-Nps/PEG. PEG is a great option because of its many distinctive qualities. Blends of polymers mix the characteristics of the separate polymers. FTIR results show intermolecular hydrogen bonding between Alg-Nps/PEG binary blend. Morphological and cross-sectional studies were analyzed using SEM. Various parameters impacting the Cu(II) ion adsorption, including pH, contact time, and adsorbent concentrations, have been examined in a batch adsorption method utilizing an Alg-Nps/PEG binary blend. Pseudo-first order, pseudo-second order, and intra particle Weber-Morris diffusion parameters have been determined. The experimental data fit the pseudo-second order kinetics model quite well when compared to the pseudo first order and intra-particular diffusion models.

[**Keywords**: Adsorption, Alginate, Blend, Kinetics model]

Introduction

Due to the fact metals are dangerous even in little amounts, heavy metal ions must be eliminated using new technology from wastewater streams from mineral sectors. Adsorption by naturally existing materials is one of the most efficient and affordable way to remove tiny amounts of heavy metal ions[1]. It has been reported to use a variety of techniques, including controlled gellification, emulsifying, interfacial polymerization and solvent evaporation. One of these techniques, controlled gellification[2-4] is particularly vulnerable to the concentration of nanoparticle constituents; therefore special expertise is required to produce aggregates with nano-sized dimensions[5]. Alginate, among other researched biopolymers like chitosan, starch, and cellulose has exceptional and extraordinary qualities that explain its capacity to form spheres and nanoparticles[6-8]. Alginate is nontoxic and biodegradable natural polysaccharide. It has undergone substantial research for use in pharmaceutical and biological products[9]. This is known to have a very high affinity for divalent metal ions and is made up of different amounts of β- 1,4 linked D-Mannurinic acid (M) and L-guluronic acid (G)[10].

Polyethylene glycol is also known as polyethylene oxide (PEO), depending on its molecular weight, and is sold under the trade name Carbowax. PEG is a great option because of its many distinctive qualities. Blended polymers combine the characteristics of distinct polymers. For instance, a synthetic polymer with strong mechanical properties, biodegradability, and biocompatibility can be used to compensate for the poor mechanical performance of a biopolymer. Depending on their molecular weights, PEG and PEO are liquids or low-melting solids[11]. Because polymer blending uses common technology at a reasonable cost, it is a widely utilized process whenever modification of characteristics is needed; the typical goals for creating a new combination of two or more ingredients.

Polymer is used to maximize the performance of the blend rather than substantially alter the component's qualities. Blending polymers is intended to produce materials with improved morphological, chemical, structural and mechanical properties[12].

Materials and Methods

Nice chemicals Pvt Limited supplied the Sodium Alginate that was procured, Cochin Kerala. PEG and Sodium hydroxide was brought from Central Drug House Pvt Limited. Calcium chloride dihydrate was purchased from Nice Chemicals Pvt Limited. Glutaraldehyde was brought from Nice chemicals and copper sulphate was obtained from Qualigens fine chemicals. The present study used only analytical reagent grade compounds.

Preparation of alginate nanoparticles

The cation-induced regulated gelification of alginate[13] was used to create alginate nanoparticles. Under steady swirling, 28.5 ml of sodium alginate (0.06 percent) solution was mixed with 1.5 ml of calcium chloride (36 mM). After that, the mixture is maintained for about an hour to stir.

Preparation of Alg-Nps/PEG binary blend flims

1 g of PEG was dissolved in 10 ml of H_2O. The prepared PEG solution is then stirred well with the alginate nanoparticles(gel) with crosslinking agent. Stirring process was done for 30 min. The petridish is then filled with it and dried.

Characterization

The Perkin Elmer 200 FTIR Spectrophotometer was used to record the FT-IR bands of the synthesized samples. SEM was used to analyze the morphologies of birnary blends (Alg-Nps/PEG-glu) that had been cross-linked with gluteraldehyde (HitachiS3400N).

Batch adsorption studies

Under static settings and in batch mode, the new biosorbent, altered Alg-nps/PEG, was tested for its capacity towards Cu(II) metal ions at various pH levels. 1 g of the sorbent and 100 ml of a created metal ion solution with various pH values were combined for this. The mixture was mechanically shaken in a stoppered bottle for 60 minutes at room temperature to bring it to equilibrium in an orbit shaker spinning at a constant speed of 160 rpm. The metal ion that was left in the filtrate after the sorbent was separated was identified by AAS.

By altering the amount of adsorbent used and time the solution was stirred, the extent of the metals' removal was examined independently. Atomic absorption spectroscopy was used to analyze the heavy metals following each stage of remediation.

Results and Discussions

FTIR spectral studies

FTIR is a potential method for both compound identification and quantification in a sample. This experiment was carried out to provide verified data regarding the vibrational origin of the pure Alg-Nps and Alg-Nps/PEG binary blend at different ratios. Figure 1 represents the FT-IR spectral information of the pure Alg-Nps. From the above spectral information of the Alg-Nps it is evident that the prominent peak is obtained at 3415.93 cm^{-1} corresponding to intermolecular H_2 bonded O-H stretching. A peak was obtained at 2924.09 cm^{-1} indicating the presence of CH_2 stretching. A peak obtained 2854.65 cm^{-1} may be due to the presence of C-H str in CH_2 aliphatic. Another peak obtained at 1618.28 cm^{-1} indicates asymmetrical carboxylate anion COO^- stretching. The peaks which are observed at 1448.54 cm^{-1} and 1382.96 cm^{-1} may be due to CH_2 bending and O-H bending respectively. C-O stretching was responsible for the peaks seen at different wave numbers, including 1118.71 cm^{-1}, 1039.63 cm^{-1}, 597.93 cm^{-1}, and 489.92 cm^{-1}. C-O-C linkage and C-C bending is because the sodium ions in alginate nanoparticles have taken the position of the calcium ions. The asymmetric stretching vibration

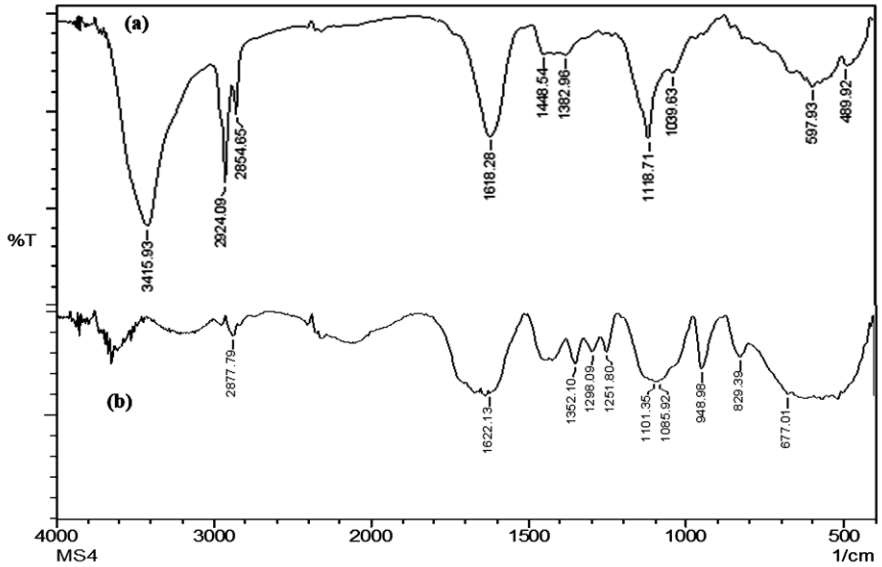

Fig. 1 — a) FTIR spectrum of pure alginate nanoparticles; and b) FTIR spectrum of Alg-nps/PEG binary blend

of the carboxylate ion has changed to a shorter wave number on comparing the Alg with pure Alg-Nps. The spectrum of Alg-Nps did not contain the characteristic sodium alginate peak at 819 cm^{-1} (Fig. 1). In placebo microgels, the absorption peak at 1624 cm^{-1} associated with the asymmetrical stretching vibration of sodium alginate changed to 1618 cm^{-1}, indicating the formation of new hydrogen bonds between -COO groups of Alg-Nps.

Figure 2 represents the FTIR spectrum of Alg-Nps/PEG(1:1)-Glu binary blend. A peak is obtained at 2877.79 cm^{-1} corresponds to CH_2 stretching. A peak is obtained at 1622.13 cm^{-1} indicates C=O asymmetrical carboxylate anion COO^- stretching, respectively. Peaks obtained at 1352.10 cm^{-1}, 1298.09 cm^{-1}, 1251.80 cm^{-1} indicates the presence of CH_2 bending vibrations and OH deformation vibration. Peaks observed at 1101.35 cm^{-1} and 1085.92 cm^{-1} may be due to the presence of C-O asymmetric and symmetric stretching and C-O-C stretching vibration. In addition, C-H bending, C-H out of plane deformation, and C-C bending are responsible for the successive maxima at 948.98 cm^{-1}, 829.39 cm^{-1}, and 677.01 cm^{-1}. Alg-Nps/vibrational PEG's shift changed when the FTIR spectral features were compared, providing evidence that the blending process was successful.

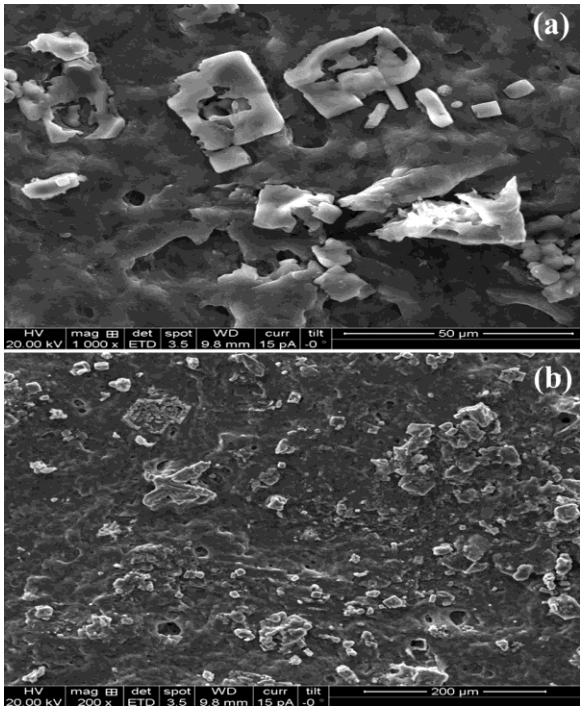

Fig. 2 — a) Morphological image of Alg-Nps/PEG (1:1)-Glu binary blend; and b) Cross-sectional views of pure Alg-Nps/PEG (1:1)-glu binary blend

Scanning Electron Microscope (SEM) analysis

The surface and pass views of the pure Alg-Nps/PEG binary blend with the cross-linking agent Gluteraldehyde is shown in Figure 2(a, b). It is evident from the micrograph that the biosorbent's surface is coarse and the majority of the granules have shrunk.

Effect of pH

Figure 3 shows effect of pH. The most significant factor affecting the sorption of metal ions on different adsorbents has been determined to be the pH of the adsorbate solutions. This is due in part to the fact that hydrogen ions are very competitive sorbates in and of themselves and in part to the fact that the pH of the solution controlled the chemical speciation of metal ions. The surface charge of the adsorbents is influenced by the pH of the solution. The copper removal percentage increases with increasing pH and reaches upto 51.67 % at 5.5 pH[14]. When the solution has a higher pH, a copper hydroxide precipitation will be the main player in the heavy metal removal process[15]. On the other hand, a drop in pH raises the concentration of hydrogen ions, which could lead to competition with metal ions for the remaining binding site[16].

Effect of contact time

Due to the presence of a greater metal ion concentration gradient and the availability of adequate vaccant adsorbing sites, a rapid initial removal rate is made achievable. Figure 4 shows the effect of contact time. As there were less accessible vacant adsorption sites, the % metal ion removal rate was reduced drastically. Due to metal ion deposition on the accessible adsorption sites on the adsorbent, further increasing the contact time had no effect on increasing the uptake[17].

Effect of adsorbent dose

Adsorbent dose is a crucial factor in determining an adsorbent's capacity for a specific starting adsorbate

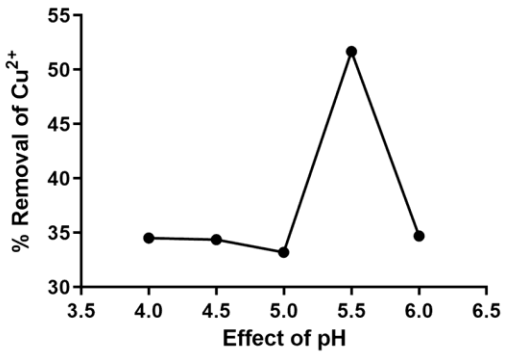

Fig. 3 — Effect of pH on the adsorption of Cu(II) ion

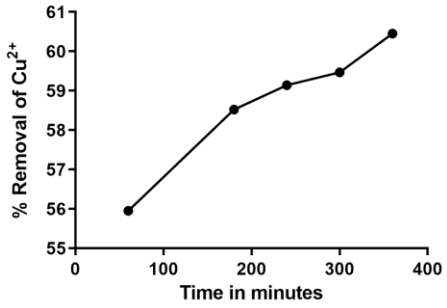

Fig. 4 — Effect of contact time on the adsorption of Cu(II) ion

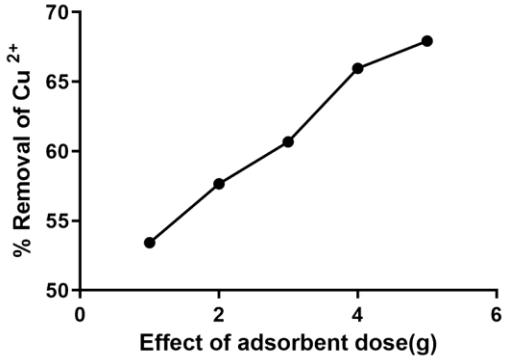

Fig. 5 — Effect of adsorbent dose on the adsorption of Cu(II) ion

concentration. Figure 5 shows the effect of adsorbent dosage. Alg-Nps/PEG dose pm Cu^{2+} removal's effect was investigated and depicted in a diagram. By adjusting the amount of adsorbents from 1 to 5 g while maintaining constant the other variables pH and contact time, the dependence of Cu(II) ion adsorption on dose was investigated. The diagram demonstrates that the rate of copper adsorption increases rapidly with an increase in the amount of Alg-Nps/PEG because there is more surfaces available at higher concentrations of the adsorbent. When the dose was increased from 2 to 4 g/100 ml, a substantial increase in absorption was seen. Beyond this, adding additional adsorbent did not significantly alter the adsorption. This might be caused by the overcrowding of adsorbent particles, which overlaps adsorption sites[18]. This finding implies that absorption peak occurs when a particular amount of adsorbent is added.

Kinetic sorption mechanisms

The pseudo-first order and pseudo-second order models can be used to quantitatively calculate and assess the adsorption rate. The treatment of natural water and waste effluents can be improved with the use of these details in additional system design applications. Rapid absorption would necessitate less time for the biosorbent and metal to come into contact, resulting in smaller equipment and lower costs. Data from kinetics and equilibrium are crucial for process design[19].

The pseudo-first-order equation

The Lagergren rate equation which is based on solid capacity, was the first rate equation for sorption in a liquid/solid system[20]. This expression can be linearized.

$$\log(qe - qt) = \log(qe) - \left(\frac{K_1}{2.303}\right) t \quad \ldots (1)$$

Where, k_1 is the rate constant of first order adsorption min^{-1}, and q_e and q_t are the amounts of Cu(II) adsorbed on the adsorbent (mg/g) at equilibrium and time t, respectively. The rate constant k_1 and the correlation coefficient R^2 values of Cu(II) under various concentration ranges were computed from the straight line plots of log (q_e -q_t) against t.

The pseudo second order equation

The pseudo second order kinetic equation is described as follows:

$$\frac{t}{q_t} = \frac{1}{k_2 . {q_e}^2} + \frac{1}{q_e} \times t \quad \ldots (2)$$

Where, k_2 is the second order adsorption's rate constant (g mg^{-1} min^{-1}). The application of this kinetic model to suit the experimental data is suggested by the straight line plot of t/qt against t, which has been evaluated to yield rate parameters.

The values of k_1 can be determined by computing the slope of the linear plot of log (q_e -$q_{t)}$ versus t, and the values of k_2 can be determined by computing the slope of the linear plot of t/qt versus t. The linear graphs of two kinetic models are displayed in Figures 6 and 7, respectively. The values of k_1, k_2, q_e, and the correlation coefficient (R^2) from the linear plots are shown in Table 1. The pseudo-second-order linear plots produced higher R_2 values than the pseudo-first-order. The q_e (cal) values from the pseudo-second-order were more similar to q_e than the values from the pseudo-first-order (exp). This illustrates the greater applicability of the pseudo-second-order model.

Intraparticle diffusion

The potential effect of intraparticle diffusion resistance on adsorption was looked at using the intraparticle diffusion model as a starting point[21].

$$q_t = K_p \, t^{\frac{1}{2}} + I \quad \ldots (3)$$

Where, K_p and I are the intraparticle diffusion rate constant (mg/g $min^{1/2}$). The graph was plotted against q_t vs $t^{1/2}$ is shown in the Figure 8.

Table 1 — Comparison between Lagergren pseudo-first-order and pseudo-second-order kinetic models for Cu(II) sorption by Alg-Nps/polyethylene glycol (1:1) – glutaraldehyde binary blend

Metal ion	Pseudo-first-order kinetic model			Experimental value	Pseudo-second-order kinetic model		
	qe (mg/g)	k_1 (min^{-1})	R^2	qe (mg/g)	qe (mg/g)	k_2 (g mg^{-1} min^{-1})	R^2
Cu(II)	305.94	$3.6*10^{-3}$	0.9361	113.44	123.45	$0.1271*10^{-2}$	0.9999

Table 2 — Intraparticle diffusion kinetic constant of adsorbent Alg-Nps/PEG binary blend

K_p	I	R^2
0.4307	53.113	0.9213

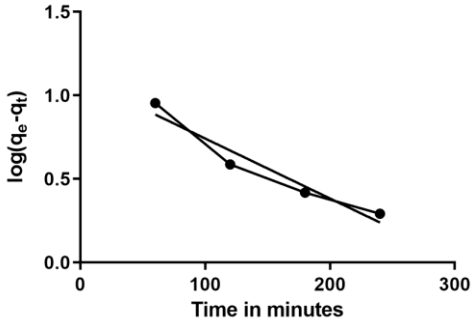

Fig. 6 — Pseudo-first-order sorption kinetic plot

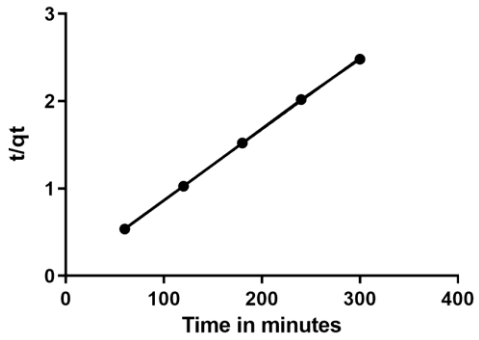

Fig. 7 — Pseudo-second-order sorption kinetic plot

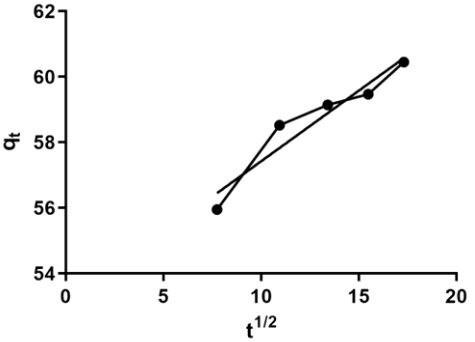

Fig. 8 — Intraparticle diffusion kinetic plot

Table 2 represents the intraparticle diffusion constant. The intraparticle diffusion kinetic model clearly plays a substantial role in the adsorption studies, as shown by the linearity of the plots R^2. Instantaneous adsorption or exterior surface adsorption was the first, sharper zone for intraparticle diffusion plots. The second zone was the stage of progressive adsorption, where intraparticle diffusion is the rate-limiting phase. There were few occurrences of the third region, or ultimate equilibrium stage, where Intraparticle diffusion began to slow down due to the dearth of adsorbate concentrations left in the fluids[22]. Figure 6 illustrates how the plots were not linear. As can be observed in Figure 6, the plots were not linear during the entire time period, indicating that many mechanisms may have affected the adsorption.

Conclusion

The adsorption of Cu(II) metal ions onto Alg-Nps/PEG binary blend was investigated in this research work. The FTIR studies reveal that the blending has taken place effectively. A kinetic model of pseudo-second order described the adsorption procedure. The outcome demonstrated that intraparticle diffusion is one of the rate-determining processes, and as a result, particle diffusion rather than film diffusion controls the adsorption process. It is also observed that more Cu(II) ions were adsorbed effectively. As a result, the current research provided a novel and highly effective adsorbent to extract heavy metals from aqueous solutions. Based on the findings, it can be said that the Alg-Nps/PEG binary mixture developed above can be employed as an adsorbent at both the laboratory and industrial levels.

Acknowledgements

The authors would like to thank the management of DKM College for Women, Vellore for extending the DST-FIST facility to carry out this research.

Conflict of Interest

The authors declare that there is no conflict of interest.

Ethical Statement

This work was not published in any mean and no endangered species are being used in this study.

Author Contributions

MS: Experimental data analysis and manuscript writing; TG: Manuscript formatting and result interpretation; SP: Plagiarism and reference formatting; AM: Data analysis and data interpretation; and PNS: Conceptualization and editing the manuscript.

References

1 Qasem Naef A A, Mohammed R H & Lawal D U, Removal of heavy metal ions from wastewater: A comprehensive and critical review, *Npj Clean Water*, 4 (1) (2021) 1-15.

2 Daemi H & M Barikani, Synthesis and characterization of calcium alginate nanoparticles, sodium homopolymannuronate salt and its calcium nanoparticles, *Sci Iran*, 19 (6) (2012) 2023-2028.

3 Sah S, Vasia M, Yadav R, Patel S & Sharma M, Microsphere Overview, *Asian J Pharm Res Dev*, 9 (4) (2021) 132-140.

4 Kumar S, Dilbaghi N, Saharan R & Bhanjana G, Nanotechnology as emerging tool for enhancing solubility of poorly water-soluble drugs, *Bionanoscience*, 2 (4) (2012) 227-250.

5 Namazi H & Mosadegh M, Bio-nanocomposites based on naturally occurring common polysaccharides chitosan, cellulose and starch with their biomedical applications, In: *Recent developments in bio-nanocomposites for biomedical applications*, edited by Tiwari A, (Nova Science Publishers, Inc), 2011, pp. 379-397.

6 Brayner R, Vaulay M-J, Fiévet F & Coradin T, Alginate-mediated growth of Co, Ni, and CoNi nanoparticles: influence of the biopolymer structure, *Chem Mater*, 19 (5) (2007) 1190-1198.

7 Stanisz M, Klapiszewski L & Jesionowski T, Recent advances in the fabrication and application of biopolymer-based micro-and nanostructures: A comprehensive review, *Chem Eng J*, 397 (2020) p. 125409.

8 Mitura S, Sionkowska A & Jaiswal A, Biopolymers for hydrogels in cosmetics, *J Mater Sci Mater Med*, 31 (6) (2020) 1-14.

9 Li J, Xiang H, Zhang Q & Miao X, Polysaccharide-Based Transdermal Drug Delivery, *Pharmaceuticals*, 15 (5) (2022) p. 602.

10 Draget K I, Skjåk-Braek G & Stokke B T, Similarities and differences between alginic acid gels and ionically crosslinked alginate gels, *Food Hydrocoll*, (2006) 20 (2-3) 170-175.

11 Reddy M S B, Ponnamma D, Choudhary R & Sadasivuni K K, A comparative review of natural and synthetic biopolymer composite scaffold, *Polymers*, 13 (7) (2021) p. 1105.

12 Nyamweya N N, Applications of polymer blends in drug delivery, *Futur J Pharm Sci*, 7 (1) (2021) 1-15.

13 Rajaonarivony M, Vauthier C, Couarraze G, Puisieux F & Couvreur P, Development of a new drug carrier made from alginate, *J Pharm Sci*, 82 (1993) 912-917.

14 Abbas S H, Ismail I M, Mostafa T M & Sulaymon A H, Biosorption of heavy metals: a review, *J Chem Sci Technol*, 3 (4) (2014) 74-102.

15 Corapcioglu M O & Huang G A, The adsorption of heavy metals onto hydrous activated carbon, *Water Res*, 21 (1987) 1031-1044.

16 Esfandiar N, Suri R & McKenzie E R, Competitive sorption of Cd, Cr, Cu, Ni, Pb and Zn from stormwater runoff by five low-cost sorbents; Effects of co-contaminants, humic acid, salinity and pH, *J Hazard Mater*, 423 (2022) p. 126938.

17 Lee A Y W, Lim S F, Chua S N, Sanaullah K, Baini R, *et al*., Adsorption equilibrium for heavy metal divalent ions (Cu^{2+}, Zn^{2+}, and Cd^{2+}) into zirconium-based ferromagnetic sorbent, *Adv Mater Sci Eng*, (2017) 1-13.

18 Guo T, Bulin C, Ma Z, Li B, Zhang Y, *et al*., Mechanism of Cd (II) and Cu (II) adsorption onto few-layered magnetic graphene oxide as an efficient adsorbent, *ACS Omega*, 6 (25) (2021) 16535-16545.

19 Revellame E D, Fortela D L, Sharp W, Hernandez R & Zappi M E, Adsorption kinetic modeling using pseudo-first order and pseudo-second order rate laws: A review, *Cleaner Eng Technol*, 1 (2020) p. 100032.

20 Kara A & Demirbel E, Kinetic, isotherm and thermodynamic analysis on adsorption of Cr (VI) ions from aqueous solutions by synthesis and characterization of magnetic-poly (divinylbenzene-vinylimidazole) microbeads, *Wat Air Soil Pollut*, 223 (5) (2012) 2387-2403.

21 Ofomaja A E, Naidoo E B & Pholosi A, Intraparticle diffusion of Cr (VI) through biomass and magnetite coated biomass: A comparative kinetic and diffusion study, *S Afr J Chem Eng*, 32 (1) (2020) 39-55.

22 Wu F C, Tseng R L & Juang R S, Initial behavior of intraparticle diffusion model used in the description of adsorption kinetics, *Chem Eng J*, 153 (1-3) (2009) 1-8.